Thermodynamical behavior of aperiodic Ising models on hierarchical lattices

R. F. S. Andrade
Instituto de Física, Universidade Federal da Bahia, 40210-340 Salvador, Brazil
(Received 20 August 1998)

This work brings an analysis of the behavior of Ising spins on a hierarchical lattice subject to relevant fluctuations on the coupling constants that are induced by a deterministic aperiodic sequence. The thermodynamical functions are evaluated after the numerical iteration of a set of coupled maps, obtained within the method of transfer matrices. The typical specific heat cusp of the homogeneous system is destroyed by the fluctuations, which also cause changes in the values of all critical exponents. [S1063-651X(99)03001-9]

PACS number(s): 05.50.+q, 64.60.Ak, 61.44.Br

I. INTRODUCTION

There has been much interest in the thermodynamical behavior and critical properties of magnetic systems with a lack of translational symmetry. Former investigations have concentrated on models defined on fractals [1], hierarchical lattices [2,3], etc., while more recent works have focused on the effect of deterministic aperiodicity in the couplings and fields that act upon the individual spins in an Euclidean lattice [4]. Of course the investigation of fully disordered or random system has proceeded along its own way, which is rather different from those we consider in this work.

Hierarchical lattices have been investigated in great detail. They are amenable to exact solutions, most of which are equivalent to approximate results for systems on Euclidean lattices. Both renormalization (decimation) schemes and the recurrent evaluation of the thermodynamical properties as the hierarchy of the lattice increases have found widespread use in these investigations [5–7].

Fully aperiodic sequences of two or more symbols are constructed by the recurrent substitution of these symbols according to a fixed rule. The sequences of Fibonacci, Thue-Morse, and Rudin-Shapiro are only a few examples of well-known aperiodic structures. Deterministic aperiodicity may be introduced by choosing couplings in a magnetic model according to the symbols in such sequences, as have already been used with success in the investigation of properties of aperiodic electronic systems [8]. The influence of the aperiodicity (or *fluctuations*) in the couplings and fields on the critical properties of the original homogeneous model is accounted for by the Luck criterion [9], which has been extended to treat also the hierarchical lattices [10]: possible changes in the critical properties depend on the eigenvalues of the substitution matrix defined by the specified inflation rule, the dimension of the lattice, and the value of one of the critical exponents (e.g., α). Fluctuations are classified into relevant or irrelevant, according to whether the critical properties are changed or not with respect to those of the homogeneous system. Situations of marginal relevance are also possible, but in such cases the criterion does not allow for a definite indication on the behavior of the system.

It is usually the case that, when fluctuations are irrelevant, the models are suitable for further analytical investigation, which ends up showing why the critical behavior remains the same [9]. However, in the case of relevant fluctuations, the analysis becomes harder and it is difficult to get a clear picture of the actual changes in the thermodynamical and critical behavior. The purpose of this work is to bring an explicit evaluation of the thermodynamical and critical properties of an Ising model on a hierarchical lattice subject to relevant fluctuations on the exchange constants. It is motivated by recent works on the same lattices within the renormalization group approach, which indicate changes in the criticality, but do not clearly point what the new behavior look like [10,11]. Our results are obtained after the numerical iteration of a set of maps for the relevant thermodynamical functions, which were derived after the use of the transfer matrix (TM) formalism. We show that changes occur in the value of all critical exponents, especially in the specific heat, which shows a completely different behavior with respect to that of the homogeneous system. In order to test our method we have reproduced the known results for the uniform model on the simple diamond lattice, and also analyzed one situation where irrelevant fluctuations do not alter the character of the criticality.

The rest of the work is organized as follows: In Sec. II we introduce the definition of the two lattices and of the fluctuation rules; in Sec. III we discuss the basic steps within the transfer matrix method that are necessary to derive the proper maps; Sec. IV presents the results for both lattices, with special emphasis on the case of relevant fluctuations; finally, Sec. V closes with concluding remarks.

II. APERIODIC MODELS ON HIERARCHICAL LATTICES

We consider an Ising model on hierarchical lattices, which are recursively constructed by substituting any bond of a given generation by a set of q parallel branches, each one containing a series of p bonds. Within this definition, the simplest diamond lattice corresponds to the situation $p=q=2$. A formal Hamiltonian for the system is written as

$$H=-\sum_{(i,j)} J_{ij}\sigma_i\sigma_j-h\sum_i \sigma_i, \tag{2.1}$$

where $\sigma_i=\pm 1$, the double sum (i,j) is performed over pairs of first-neighbor sites, and h is a uniform field acting on all sites of the lattice. We choose rules for the bonds J_{ij} such that any path linking the two root points (points which appear in the first generation) has the same sequence of bonds. The length of these paths is given by p^G, where G indicates the generation of the construction of the lattice. For conve-

nience we choose rules for the sequences governing fluctuations the lengths of which have the same dependence on G. We consider substitution rules formed by only two symbols (A and B), generically expressed by

$$(A,B)\rightarrow(AB^{p-1},A^{p}), \tag{2.2}$$

and the sequences start with a single symbol A. We assume that the nearest-neighbor interactions J_{ij} in our model assume the values J_A or J_B according to the symbol in the sequence.

The substitution matrix M, which links the number of symbols A and B in two subsequent generations is written as

$$M=\begin{pmatrix} 1 & p \\ p-1 & 0 \end{pmatrix}. \tag{2.3}$$

Its eigenvalues are $\lambda_1=p$ and $\lambda_2=1-p$, and they define the wandering exponent

$$\omega=\frac{\ln|\lambda_2|}{\ln\lambda_1}. \tag{2.4}$$

ω expresses whether the fluctuations in the distribution of symbols within the sequence are bounded ($\omega<0$) or unbounded ($\omega>0$). The sequences defined by Eq. (2.2) are non-Pisot (i.e., $\omega>0$) for $p>2$, whereas $\omega=0$ for $p=2$. The extension of the Luck-Harris criterion for relevant fluctuations in the case of hierarchical lattices leads to the expression [10]

$$\phi=1-\omega-\frac{d_f}{2-\alpha}<0, \tag{2.5}$$

where the fractal dimension is expressed by $d_f=[\ln(pq)/\ln(p)]$, and α is the specific heat exponent of the uniform system.

In the following sections we focus on two situations where $d_f=2$: $p=q=2$ and 3. The analysis of renormalization group [10] has shown that, for any value of q, $\phi>0$ when $p=2$, even if $\omega=0$, while $\phi<0$ when $p=3$. Besides that, the same analysis shows that the nature of the fixed point associated with the $T\neq0$ transition changes from an unstable node (with one attractive and one repulsive eigenvector) to a completely repulsive situation. The new properties of the fixed point make it hard to get an indication about the nature of the transition and the thermodynamical behavior of the aperiodic system. So we can only obtain information about the nature of the changes induced by relevant fluctuations by the explicit evaluation of the thermodynamical properties of the system.

III. TRANSFER MATRIX FORMULATION

TM's were first devised for the analysis of translationally invariant systems. However, they have been used recently in connection with deterministic aperiodic [8,12] and random [13] systems as well as on the analysis of fractals with finite order of ramification [14]. The approach we use in this work combines elements of both quoted schemes.

For the sake of simplicity we start with the homogeneous case and no external field. When $G=0$ the system reduces to a single bond between the root sites r_1 and r_2. A usual 2×2 matrix T_0 with Boltzmann weights describes the interaction J between the root points. In the next generation, the interaction between sites r_1 and r_2 is expressed by a 2×2 matrix T_1 given by

$$T_1=Q_0R_0^{p-2}Q_0^{t}. \tag{3.1}$$

In Eq. (3.1) the matrix R_0 describes the bonds between the inner new sites of the first generation. It is expressed as Kronecker direct products of q 2×2 matrices of Boltzmann weights T_0. The matrix Q_0 describes the interaction of the root site r_1 with the first inner sites of the q branches. It is a 2×2^q matrix, formed by the first and last lines of the matrix T_0. Its transpose Q_0^t describes the interaction of the last q inner sites with the root site r_2.

Through Eq. (3.1) we relate matrix elements of two successive generations of the lattice. In such a simple case, T_0 and T_1 contain only two distinct matrix elements, say a_0,b_0 and a_1,b_1, which are related by nonlinear maps.

Due to exact scale invariance of the lattice, the matricial map (3.1) relates the TM's of any two subsequent generations G and $G+1$. The same is valid for the maps for the matrix elements. They can be iterated in a more convenient way if we introduce the free energy per spin $f_G=-(T/N_G)\ln\eta_G$, and the correlation length $\xi_G=p^G/\ln(\eta_G/\epsilon_G)$, where $\eta_G=a_G+b_G$ and $\epsilon_G=a_G-b_G$ are the eigenvalues of the matrix T_G, and N_G counts the number of sites of the lattice in the generation G. For $p=q=2$ and 3 we have, respectively, $N_G=2(2+4^G)/3$ and $N_G=(5+3\times9^G)/4$. The explicit forms for the maps for $p=q=2$ and 3 are

$$f_{G+1}=\frac{4N_G}{N_{G+1}}f_G-\frac{T}{N_{G+1}}\{\ln2-\ln[1+\exp(-4\times2^G/\xi_G)]\};$$

$$\xi_{G+1}=\xi_G\left\{1+\frac{\xi_G}{2^{G+1}}[\ln[1+\exp(-4\times2^G/\xi_G)]-\ln2]\right\}^{-1}; \tag{3.2}$$

$$f_{G+1}=\frac{9N_G}{N_{G+1}}f_G-\frac{T}{N_{G+1}}\{\ln4-\ln[1+3\exp(-6\times3^G/\xi_G)]\};$$

$$\xi_{G+1}=\xi_G\left\{1+\frac{\xi_G}{3^{G+1}}\left[\ln\left(\frac{1+3\exp(-6\times3^G/\xi_G)}{3+\exp(-6\times3^G/\xi_G)}\right)\right]\right\}^{-1} \tag{3.3}$$

The iteration of Eq. (3.2), [(3.3)] leads to the numerical exact value of the corresponding thermodynamic functions. The entropy and specific heat are evaluated in the same way, after the derivation of the maps for $\partial f_{G+1}/\partial T$ and $\partial^2 f_{G+1}/\partial T^2$.

To include the effect of a homogeneous field on the spins we disregard, for $G=0$, the field acting on the root sites. In the evaluation of T_1 we include the field effect only on the inner sites, and repeat this procedure for all further generations. In the limit $G\rightarrow\infty$ we have included exactly the same field intensity in all sites, with exception of the two root sites

that remain field free. With the inclusion of the field the eigenvalues η_G and ϵ_G are not any more linear combination of the now three distinct matrix elements of matrices T_G. This makes the corresponding maps for f_G and ξ_G more complex. The magnetization and susceptibility as function of the generation G are obtained by derivation of these field-dependent maps with respect to h.

Finally we discuss the inclusion of aperiodicity for substitution rules that include only two symbols, as those defined by Eq. (2.2). Suppose that the hierarchy starts with a single bond of type A, described by the TM $T_{A,0}$, of Boltzmann weights defined with the coupling J_A. The matrix $T_{B,0}$ with coupling J_B is constructed in the same way. To express the interactions at second and higher order generations we need two matrix relations of the type (3.1) for $T_{A,1}$ and $T_{B,1}$, which are formally written as

$$T_{x,1}=Q_{x,0}\left[\prod_{k=1}^{p-2} R_{x_k,0}\right]S^t_{x,0}, \quad x=A,B. \tag{3.4}$$

The matrices Q, R, and S have the same meaning as in Eq. (3.1) but we have to take into account the type of coupling (J_A or J_B) according to the substitution rule for the matrices A and B. This is the only relevant change in the procedure, which amounts to maps for the matrix elements of A and B. The inclusion of the external field is made in the same way as for the uniform case. In general there will be four different maps for the matrix elements of each matrix. The complete set of maps for the aperiodic situations analyzed here, with inclusion of magnetic field, are listed in the Appendix.

IV. RESULTS

The maps have been iterated with double precision variables until a relative precision of 10^{-16} in the values of the different quantities is achieved. To test the method we have reproduced the known results for the homogeneous diamond lattice, $J_A=J_B>0$, $p=q=2$, where we found the critical temperature to be $T_c=1.641\,017\,9\ldots$. The best estimate for T_c is obtained by gradually reducing T from the high value region and observing where ξ diverges. The iteration of the maps shows that $\xi\to\infty$ for all $T<T_c$. At T_c we also observe the criticality for the specific heat c, the curve of which has the form of a cusp, with maximum $0.959\,763\,0\ldots$.

The evaluation of the spontaneous magnetization m_0 has to be performed in the limit $h\to 0$, since if we set $h=0$ in the beginning of the iteration we end up with $m\equiv 0$. For $T>T_c$, high precision values for $m=m(T,h\ll 1)\simeq m_0$, with error $<10^{-8}$, are obtained for $h\sim 10^{-10}$ when $t=(T-T_c)/T_c>0.01$. For $t<0.01$ we have to take still smaller values of h in order to achieve convergence. For $T>T_c$, m falls initially along the same way as for $T<T_c$, as the critical temperature $T_c(h)$ is somewhat larger than T_c. We have estimated that

$$t_c(h)=\frac{T_c(h)-T_c}{T_c}\simeq 0.44h^{0.38}. \tag{4.1}$$

After reaching $T_c(h)$, m falls very rapidly with t, according to a power law with exponent ~ 2.24. If we fix the value of $T>T_c(h_0)$, we note that $m\sim h^{-1}$ for $h<h_0$. For instance we note that, for the value of T_c listed above, m drops from the value 0.252 at $T_c-0.0001$ to 0.164 at $T_c+0.0001$ for $h=10^{-10}$ and from 0.247 to 3.3×10^{-4} when $h=10^{-14}$.

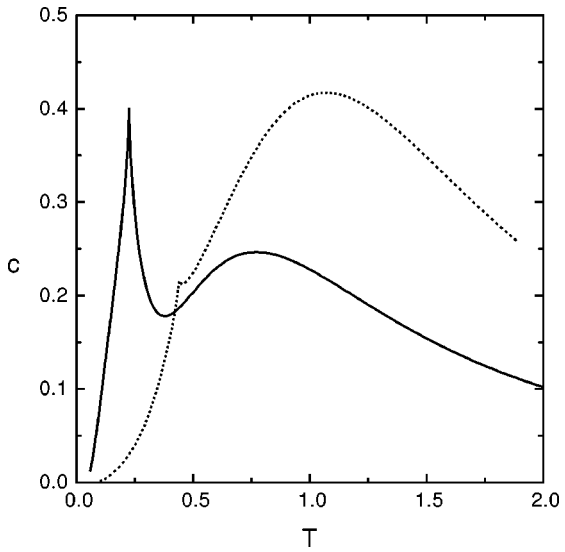

FIG. 1. Specific heat for the simple diamond lattice ($p=q=2$) for the coupling constants $J_A=0.1$, $J_B=1$ (solid curve) and $J_A=1$, $J_B=0.1$ (small dashed). The critical exponent α remains invariant.

For $T<T_c$ the zero-field susceptibility χ_0 diverges at T_c, but the convergence of $\chi(T,h)$ to χ_0 when $h\to 0$ is not so precise as for m. Results for $h\sim 10^{-10}$ have relative precision of 10^{-6} but, due to rounding off errors, the convergence of $\chi(T,h)$ to χ_0, for still smaller fields becomes poor, especially for T far from T_c. For $T>T_c$ we observe that the value of the susceptibility is finite for nonzero h. However they do not evolve to a fixed value, but diverge with $|\ln h|$ in the $h\to 0$ limit [15,16]. This behavior is in accordance with analytical results, which show that χ_0 is infinite for $T>T_c$. The numerical values for the critical exponents are also reproduced with high accuracy: $\alpha=-0.672$, $\beta=0.1617$, $\gamma=2.351$, $\nu=1.338$.

The same procedure was repeated for several pairs of values of $J_A, J_B>0$. Besides the change in T_c, the value of which for $J_A\neq J_B$ could not be obtained within the renormalization group approach, we have checked that the critical exponents remain invariant, indicating that the critical behavior are the same as in the homogeneous situation. Other relevant changes in the thermodynamical behavior are observed in the curve for c: in the limit of small J_B the cusp at T_c has its size reduced and becomes embedded within a Schottky profile that dominates the greater part of the curve; in the limit of small J_A the cusp still dominates, but a small Schottky profile develops for $T>T_c$, as shown in Fig. 1.

We expect changes is the critical behavior when fluctuations in the coupling constants are introduced in the second lattice, $p=q=3$. The homogeneous situation presents the same qualitative features of the standard diamond lattice. When $J_A=J_B$ we have found $T_c=1.385\,391\,2\ldots$, and the maximum of the cusp for c at $0.930\,733\,5\ldots$. The critical exponents are $\alpha=-0.701$, $\beta=0.168$, $\gamma=2.356$, $\nu=1.354$, which, like the estimates for the diamond lattice, satisfy the Rushbrook and hyperscale relations to a high pre-

cision, with errors less than 0.3%.

When $J_A \neq J_B$ both qualitative and quantitative changes are observed, respectively, in the critical behavior of c and in the critical exponents ν, β, and γ.

The critical temperature T_c is again estimated by the divergence of ξ. For instance, when $J_A=1$ and $J_B=0.2$ we have $T_c=0.409\,066\,938\ldots$. As in all former cases, ξ presents a clear power-law behavior for a large interval of t. We measured a new value $\nu=1.485$, which remains invariant as long as $J_A \neq J_B$.

We also find that in the limit $h \to 0$, $m_0 \simeq m \to 0$ when $T \to T_c$, with a new universal value $\beta=0.067$ for $J_A \neq J_B$. As we must perform the evaluation of m with a small nonzero h, the former discussion on the behavior of $m \simeq m_0$ applies to the present situation. The convergence of m to m_0 is much slower than in the uniform case or in the presence of irrelevant fluctuations. Our estimates are that

$$t_c(h)=\frac{T_c(h)-T_c}{T_c} \simeq 7.3h^{0.35}. \tag{4.2}$$

So, for the values of J_A and J_B quoted above, m_0 drops from 0.587 at $T_c-0.0001$ to 0.122 at $T_c+0.0001$ when $h=3\times10^{-14}$, and from 0.587 to 2.24×10^{-3} when $h=3\times10^{-16}$. As the numerical variables we work with are limited to 16 significant digits, this is the smallest value of h for which $t_c(h)$ could be obtained with confidence. Finally we note that for $T>T_c(h)$, m decays according to a power law with t; the exponent (~ 2.54) is even larger than in the uniform case. The main features of the analysis of our data are shown in the Figs. 2(a) and 2(b).

The behavior of χ_0 for $T<T_c$ has now a steeper divergence.The scaling region is large, but we note that the constant steep slope suffers a slight break at an intermediate point, returning afterwards to the same steep decay [see Fig. 2(c)]. This effect must be of the same nature as the log-periodic oscillations detected in connection to the specific heat, as we discuss below. If we measure the slope in any of the two steeper parts, we come to the same result $\gamma \simeq 2.72$. When $T>T_c$ the inhomogeneous model also have infinite zero field susceptibility, which diverges for small h as $\ln h$.

The fact that these three thermodynamical functions have the same qualitative behavior as the uniform model is important to characterize the nature of the critical behavior at T_c. We think that the overall picture fits into the framework of a second-order transition, even if the criticality in the specific heat suffers the destruction of the cusp. As shown in Fig. 3, the curve now displays a smooth maximum at $T_m<T_c$, such that $t_m=|T_m-T_c|/T_c \sim 10^{-3}$. At $T=T_c$ the curve suffers a discontinuous change in its derivative, suggesting that the critical behavior is of the type

$$\begin{aligned} c(T)&=c_0+c_1(T_c-T)^{\alpha}, \quad \text{for} \quad T<T_c, \\ c(T)&=c_0-c_1'(T-T_c)^{\alpha'}, \quad \text{for} \quad T>T_c, \end{aligned} \tag{4.3}$$

with $\alpha \neq \alpha'$. For $T<T_c$, the interval where Eq. (4.3) is valid is reduced to $t<t_m$. As t_m is rather small the evaluation of α is restricted to a very narrow interval around $t=0$. Note that the numerical fluctuations become more relevant as t decreases. Therefore the value of α cannot be estimated with the same precision as the first three exponents. When $T>T_c$ we do not have a limitation for the interval where scaling occurs. The double logarithm plot of ct shows that the points align along a straight line, although a careful analysis show that there are some fluctuations [Fig. 3(d)] of the same kind as those observed for the susceptibility. The best estimates for the values of the exponents are $\alpha=-0.80$ and $\alpha'=-0.89$.

In order to provide a closer analysis of the fluctuations in the behavior of $c(T)$ for $T \sim T_c$ we have evaluated its derivative dc/dT, which is shown in Fig. 4. The most relevant aspect is the log-periodic oscillations of dc/dT with respect to the reduced temperature t for $T>T_c$. An indication of a similar behavior is also obtained for m and χ. However, since these quantities, respectively, vanish and diverge at T_c, the effect can only be depicted if we compute the logarithmic derivative. Log-periodic phenomena has also been reported for magnetization and free energy of the mean field approximation of an aperiodic system [17], when $T<T_c$. We observe that the period of oscillation is roughly equal to the wandering exponent (2.4) $\omega=\ln 2/\ln 3 \simeq 0.64$. So we can relate the oscillations to the increase of disorder in the successive hierarchies of aperiodicity induced by the sequence. We also note that, to accurately describe such an effect, the form (4.3) we assumed for the dependence of c for $T>T_c$ should a log-periodic function be included. However, the amplitude of fluctuation is so minute that it does not alter substantially the obtained values for the critical exponents. Another relevant feature of the curve in Fig. 4 is the slow increase of the quantity $(dc/dT)_{T=T_c-\Delta}-(dc/dT)_{T=T_c+\Delta}$ as $\Delta \to 0$, if we average dc/dT over the period of oscillations. This is consistent with the form (4.3) and with the values obtained for α and α'.

The numerical estimation for the critical exponents leads to

$$\begin{aligned} \alpha+2\beta+\gamma-2 &\simeq 0.05, \\ \alpha'+d_f\nu-2 &\simeq 0.08. \end{aligned} \tag{4.4}$$

This result is worse than that obtained for the uniform models. It is not possible to assert whether it depends on the employed method or it is an essential feature of the model, caused by the presence of relevant fluctuations.

V. CONCLUSIONS

In this work we have evaluated the thermodynamical functions of an aperiodic Ising system on hierarchical lattices through the numerical iteration of a set of maps. The important issue was to uncover the nature of the transition and of the thermodynamical behavior of a system subject to *relevant fluctuations* in the coupling constants, as is the case of the hierarchical lattice with $p=q=3$ subject to the fluctuations induced by the inflation rule (2.2). For such system, the relevant character of the fluctuations has been established by a renormalization group analysis. The same study shows that the fixed point associated with the transition at $T \neq 0$ becomes a fully unstable node (two repulsive eigenvectors). The elimination of the attractive manifold of the fixed point fact makes it hard to get a picture of what the transition looks

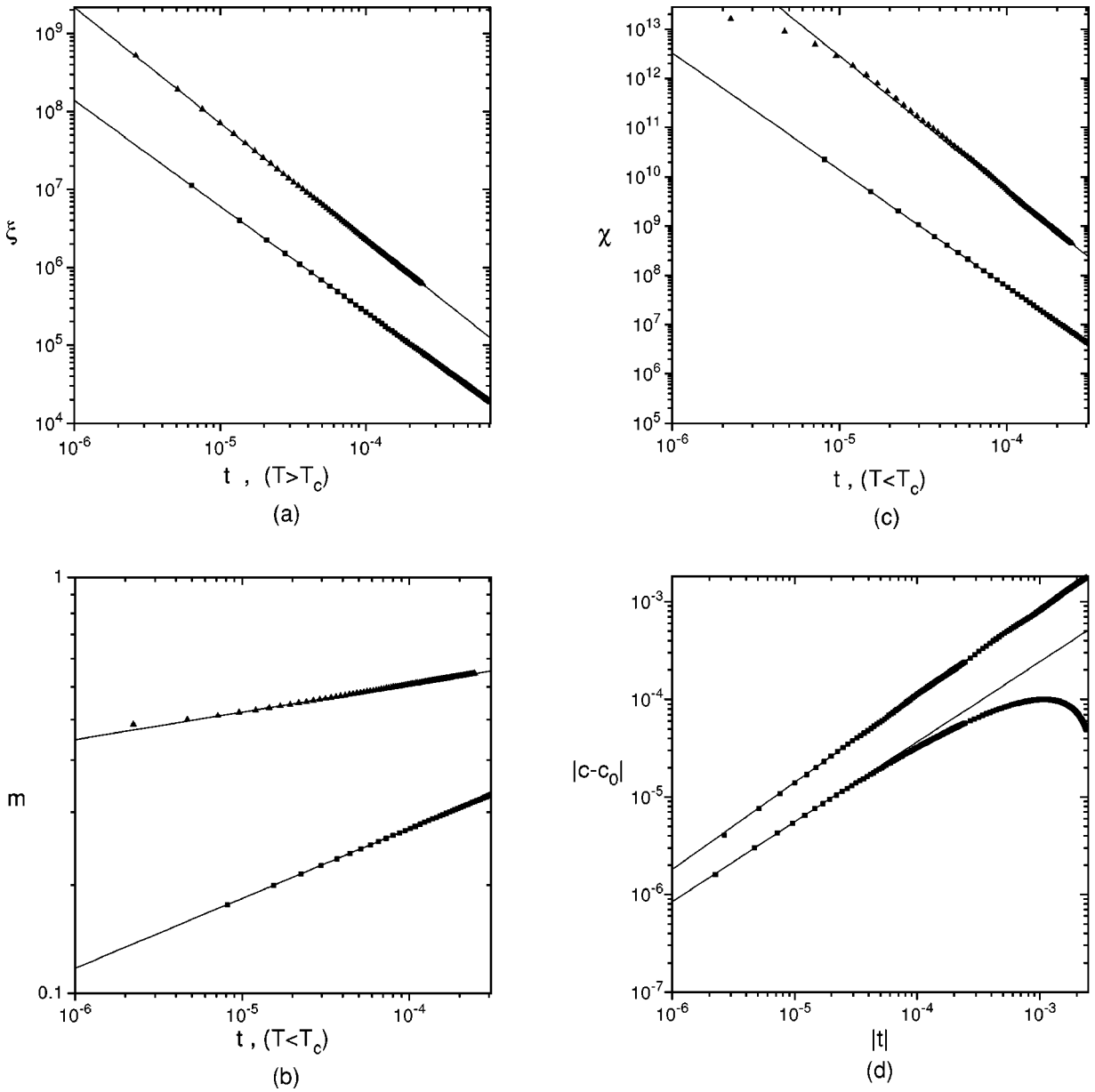

FIG. 2. Scaling properties of correlation length ξ (a), magnetization m, and susceptibility χ in the $h\to 0$ limit (b) and (c) with respect to the reduced temperature t. The squares indicate the uniform case $J_A=J_B=1$, and the triangles indicate $J_A=1$, $J_B=0.2$. The new values for the slopes remain constant as long as $J_A\neq J_B$. In (d) we plot the specific heat for both $T<T_c$ (lower branch) and $T>T_c$. The small irregularities in the upper branch are magnified in Fig. 4.

like, as we can never approach the fixed point through the iteration of the renormalization transformations. Conjectures that the second-order character of the transition be lost can be raised in such cases.

The picture described above is typical also for other situations where relevant fluctuations have been considered. The analytical methods cannot be further developed and a definitive statement about the behavior of the system remains far off. The elucidation of these points demands the exact evaluation of the thermodynamical functions of the system.

The results we present here are numerically exact, as the maps we iterate were derived without any approximation. However they are subject to rounding off errors in the iteration of the maps and imprecision in the fitting for the critical exponents. As shown in the last section, the numerical estimates for the critical temperature and exponents for both uniform models and the situation of irrelevant fluctuations are of quite good quality, which attests to the reliability of our method.

The relevant fluctuations have induced quantitative changes in the values of the exponents ν, β, and γ. However, the new values are universal as long as $J_A=J_B$. We have observed that the critical temperature T_c estimated by the divergence of ξ agrees to high precision with those where $m_0\to 0$ and $\chi_0\to\infty$. The scaling region is large for the three exponents, and high precision values were obtained for the first two of them. In the evaluation of γ, we have observed that the points do not align so precisely along a straight line as the former two exponents, which is the reason for a larger error.

The most relevant change refers to the destruction of the specific heat cusp. A complex behavior develops, character-

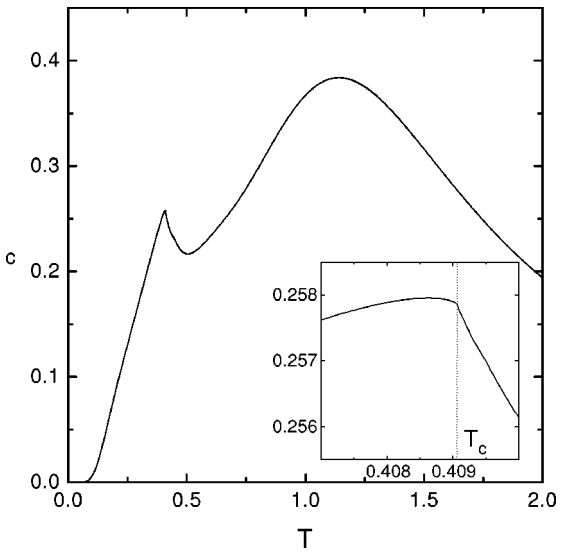

FIG. 3. Specific heat c for $J_A=1$, $J_B=0.2$. The inset is a magnification of the region around T_c. Note the smooth maximum at T_m and the change in the slope at T_c.

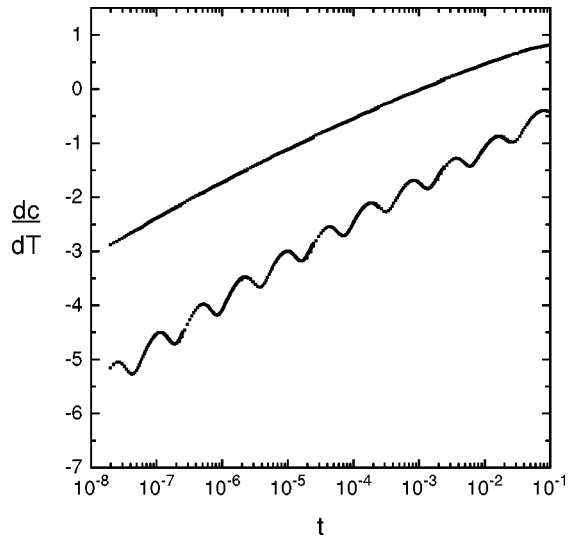

FIG. 4. Curve for (dc/dT) vs t for both $T<T_c$ (upper branch) and $T>T_c$. Note that the slight increase in the distance between the two curves as $t\to 0$. This divergence is consistent with the expression (4.3). The period of the oscillations of the lower branch $\sim \ln 2/\ln 3$.

ized by a smooth maximum at a temperature T_m slightly smaller than T_c, and a change in the derivative of c with respect to T at T_c, which can only be interpreted as a manifestation of the same criticality that causes the divergence of ξ and χ_0 and the vanishing of m_0. We emphasize that the detailed numerical investigations shows clearly the existence of the two distinct values T_m and T_c, and that the difference between these two values is much larger than the deviation found in the values of the temperatures at which the criticality sets in the different functions. So we can definitely rule out that two temperature values are an artifact due to numerical imprecision. The complex behavior is further characterized by small changes in the slope of c when $T>T_c$. This effect is clearly shown in the curve of dc/dT, which displays log-periodic oscillations with respect to the reduced temperature. We found that the period is approximately given by the wandering exponent of the aperiodic sequence controlling the fluctuations.

We also call attention to the fact that the entropy varies continuously through the entire temperature interval. We have carried out a detailed investigation of its behavior around the critical region, but could not observe any evidence for a discontinuous change, which would provide evidence for a first-order transition.

To conclude we stress that the detailed numerical evaluation of the thermodynamical behavior of a system subject to relevant fluctuations does support the survival of the second-order transition, though characterized by new universal critical exponents ν, β, and γ, and the presence of a discontinuity in the slope of the specific heat at T_c.

ACKNOWLEDGMENTS

The author is greatly indebted to Professor S.R. Salinas for helpful discussions and a critical reading of the manuscript, and to S.T.R. de Pinho and T. Haddad for adding useful observations to some of our results and to the current literature on the subject.

APPENDIX

Maps for the free energy $f_G(T,h)$ and the correlation length $\xi_G(T,h=0)$ for the hierarchical lattice with $p=q=2$.

$$f_{G+1}=2\frac{N_G}{N_{G+1}}(f_G+g_G)-\frac{T}{N_{G+1}}\ln\left(\frac{A_G}{4}\right),$$

where the recurrence for g_G is given by

$$g_{G+1}=4\frac{N_G}{N_{G+1}}f_G-\frac{T}{N_{G+1}}\ln\left(\frac{B_G}{4}\right).$$

The terms A_G and B_G are further expressed by

$$\begin{aligned}A_G=&(1-x_G^2-y_G^2+z_G^2)(1-u_G^2)\\&+\frac{H^2}{2}[(1+y_G)^2+(x_G+z_G)^2]\\&\times[(1+v_G)^2+(u_G+v_G)^2]\\&+\frac{1}{2H^2}[(1-y_G)^2+(x_G-z_G)^2]\\&\times[(1-v_G)^2+(u_G-v_G)^2],\end{aligned}$$

and

$$B_G=(1-x_G^2-y_G^2+z_G^2)^2+\frac{H^2}{2}[(1+y_G)^2+(x_G+z_G)^2]^2$$

$$+\frac{1}{2H^2}[(1-y_G)^2+(x_G-z_G)^2]^2.$$

In A_G and B_G we have $N_G=2(2+4^G)/3$ and $H=\exp(h/T)$ $(k_B=1)$. The recurrence relations for the quantities present in A_G and B_G are

$$x_{G+1}=\frac{1}{A_G}\Bigg\{4(z_G-x_Gy_G)v_G(1-u_G)+2H^2(1+y_G)(x_G+z_G)(1+v_G)(u_G+v_G)$$
$$+\frac{2}{H^2}(1-y_G)(x_G-z_G)(1-v_G)(u_G-v_G)\Bigg\};$$

$$y_{G+1}=\frac{1}{A_G}\Bigg\{2(1-x_G^2-y_G^2+z_G^2)v_G(1-u_G)+H^2[(1+y_G)^2+(x_G+z_G)^2](1+v_G)(u_G+v_G)$$
$$-\frac{1}{H^2}[(1-y_G)^2+(x_G-z_G)^2](1-v_G)(u_G-v_G)\Bigg\};$$

$$z_{G+1}=\frac{1}{A_G}\Bigg\{2(z_G-x_Gy_G)(1-u_G^2)+H^2(1+y_G)(x_G+z_G)[(1+v_G)^2+(u_G+v_G)^2]$$
$$-\frac{1}{H^2}(1-y_G)(x_G-z_G)[(1-v_G)^2+(u_G-v_G)^2]\Bigg\};$$

$$u_{G+1}=\frac{1}{B_G}\Bigg\{4(z_G-x_Gy_G)^2+2H^2(1+y_G)^2(x_G+z_G)^2+\frac{2}{H^2}(1-y_G)^2(x_G-z_G)^2\Bigg\};$$

$$v_{G+1}=\frac{1}{B_G}\Bigg\{2(1-x_G^2-y_G^2+z_G^2)(z_G-x_Gy_G)+H^2[(1+y_G)^2+(x_G+z_G)^2](1+y_G)(x_G+z_G)$$
$$-\frac{1}{H^2}[(1-y_G)^2+(x_G-z_G)^2](1-y_G)(x_G-z_G)\Bigg\}. \tag{A1}$$

The initial conditions for these maps are

$$f_0=-\frac{T}{2}\ln[\cosh(J_A/T)];\quad g_0=-\frac{T}{2}\ln[\cosh(J_B/T)];$$

$$x_0=\tanh(J_A/T);\quad u_0=\tanh(J_B/T);\quad y_0=z_0=v_0=0.$$

For the $\xi(T,h=0)$ the corresponding maps are

$$\xi_{G+1}=2\frac{\xi_G\zeta_G}{\xi_G+\zeta_G}\Bigg[1+\frac{2^{-G}\xi_G\zeta_G}{\xi_G+\zeta_G}\times\ln\left(\frac{1+\exp[-2^{G+1}(1/\xi_G+1/\zeta_G)]}{2}\right)\Bigg]^{-1},$$

where the variable ζ_G follows the recurrence relation:

$$\zeta_{G+1}=\xi_G\left[1+2^{-G-1}\xi_G\ln\left(\frac{1+\exp(-2^{G+2}/\xi_G)}{2}\right)\right]^{-1}.$$

The initial conditions are

$$\xi_0=\frac{-1}{\ln[\tanh(J_A/T)]};\quad \zeta_0=\frac{-1}{\ln[\tanh(J_B/T)]}.$$

Maps for the free energy $f_G(T,h)$ and the correlation length $\xi_G(T,h=0)$ for the hierarchical lattice with $p=q=3$ are

$$f_{G+1}=3\frac{N_G}{N_{G+1}}(f_G+2g_G)-\frac{3T}{N_{G+1}}\ln(A_G),$$

where the recurrence for g_G is given by

$$g_{G+1}=9\frac{N_G}{N_{G+1}}f_G-\frac{3T}{N_{G+1}}\ln(B_G).$$

The terms A_G and B_G are further expressed by

$$A_G=H^4+u_G^2+x_Gv_G+x_Gu_Gw_GH^{-4};$$

$$B_G=H^4+x_G^2+x_Gy_G+x_G^2z_GH^{-4}.$$

In A_G and B_G we have $N_G=(5+3\times9^G)/4$ and H has the same meaning as before. The recurrence relations for the quantities present in A_G and B_G are

$$x_{G+1}=\frac{1}{A_G^3}\{v_GH^4+x_Gv_G^2+u_Gw_G+x_Gw_G^2H^{-4}\}^3;$$

$$y_{G+1}=\frac{1}{A_G^3}\{y_GH^4+y_Gu_G^2+z_Gv_G+z_Gu_Gw_GH^{-4}\}^3;$$

$$z_{G+1}=\frac{1}{A_G^3}\{y_Gv_GH^4+z_Gv_G^2+y_Gu_Gw_G+z_Gw_G^2H^{-4}\}^3;$$

$$u_{G+1}=\frac{1}{B_G^3}\{y_G H^4+x_G y_G^2+x_G z_G+x_G z_G^2 H^{-4}\}^3;$$

$$v_{G+1}=\frac{1}{B_G^3}\{y_G H^4+x_G^2 y_G+y_G z_G+x_G z_G^2 H^{-4}\}^3;$$

$$w_{G+1}=\frac{1}{B_G^3}\{y_G^2 H^4+x_G y_G z_G+y_G^2 z_G+z_G^3 H^{-4}\}^3.$$

The initial conditions are

$$f_0=-\frac{J_A}{2};\quad g_0=-\frac{J_B}{2};\quad x_0=y_0=\exp(J_A/T);$$
$$u_0=v_0=\exp(J_B/T);\quad z_0=w_0=1.$$

For the $\xi(T,h=0)$ the corresponding map is

$$\xi_{G+1}=3\frac{\xi_G\zeta_G}{\xi_G+\zeta_G}\left[1+\frac{3^{-G}\xi_G\zeta_G}{\xi_G+2\zeta_G}\times\ln\left(\frac{1+3\exp[-3^G(2/\xi_G+4/\zeta_G)]}{3+\exp[-3^G(2/\xi_G+4/\zeta_G)]}\right)\right]^{-1},$$

where the variable ζ_G follows the recurrence relation:

$$\zeta_{G+1}=\xi_G\left[1+3^{-G-1}\xi_G\ln\left(\frac{1+3\exp(-6\times3^G/\xi_G)}{3+\exp(-6\times3^G/\xi_G)}\right)\right]^{-1}.$$

The initial conditions for ξ_0 and ζ_0 are the same as for $p=q=2$.

[1] First reference on the subject is Y. Gefen, B. B. Mandelbrot, and A. Aharony, Phys. Rev. Lett. **45**, 855 (1980); A vast literature on magnetic models on fractals is now available.
[2] A. N. Berker and S. Ostlund, J. Phys. C **12**, 4961 (1979).
[3] M. Kaufman and R. B. Griffiths, Phys. Rev. B **24**, 496 (1981).
[4] U. Grimm and M. Baake, in *The Mathematics of Long Range Aperiodic Order*, edited by R. V. Moody (Kluwer Academic, Amsterdam, 1997), pp. 199–237.
[5] J. R. Melrose, J. Phys. A **16**, 1041 (1983); **16**, 3077 (1983).
[6] R. B. Griffiths and M. Kaufman, Phys. Rev. B **26**, 5022 (1982); M. Kaufman and R. B. Griffiths, *ibid.* **30**, 244 (1984).
[7] C. Tsallis and A. C. N. de Magalhães, Phys. Rep. **268**, 305 (1996).
[8] M. Kohmoto, L. P. Kadanoff, and C. Tang, Phys. Rev. Lett. **50**, 1870 (1983); S. Ostlund, R. Pandit, D. Rand, H. J. Schellnhuber, and E. D. Siggia, *ibid.* **50**, 1873 (1983).
[9] J. M. Luck, Europhys. Lett. **24**, 359 (1993); J. Stat. Phys. **72**, 417 (1993).
[10] S. T. R. de Pinho, T. A. S. Haddad, and S. R. Salinas, Braz. J. Phys. **27**, 567 (1997); Physica A **257**, 515 (1998).
[11] A. C. N. de Magalhães, S. R. Salinas, and C. Tsallis, J. Phys. A **31**, L567 (1998).
[12] R. F. S. Andrade and H. S. Schellnhuber, Europhys. Lett. **10**, 73 (1989).
[13] A. Crisanti, G. Paladin, and A. Vulpiani, *Products of Random Matrices in Statistical Physics* (Springer-Verlag, Berlin, 1996).
[14] R. F. S. Andrade, Physica A **193**, 29 (1993); Phys. Rev. B **48**, 16 095 (1993).
[15] P. M. Bleher and E. Zalys, Commun. Math. Phys. **120**, 409 (1989).
[16] M. Kaufman and R. B. Griffiths, J. Phys. A **15**, L239 (1982).
[17] P. E. Berché and B. Berché, J. Phys. A **30**, 1347 (1997).